75th International Astronautical Congress (IAC), Milan, Italy, 14-18 October 2024.

IAC–24–A.3.4B.6

Scientific and Technological Objectives for the NavCam Payload of Hera's Milani CubeSat to Binary Asteroid Didymos

Iosto Fodde[a*], Alessia Cremasco[b], Felice Piccolo[c], Pietro Califano[d], Lucia Francesca Civati[e], Antonio Rizza[f], Carmine Giordano[g], Paolo Panicucci[h], Fabio Ferrari[i], Francesco Topputo[j]

[a] *Department of Aerospace Science and Technology, Politecnico di Milano, Via La Masa 34, Milano, Italy, iosto.fodde@polimi.it*
[b] *Department of Aerospace Science and Technology, Politecnico di Milano, Via La Masa 34, Milano, Italy, alessia.cremasco@polimi.it*
[c] *Department of Aerospace Science and Technology, Politecnico di Milano, Via La Masa 34, Milano, Italy, felice.piccolo@polimi.it*
[d] *Department of Aerospace Science and Technology, Politecnico di Milano, Via La Masa 34, Milano, Italy, pietro.califano@polimi.it*
[e] *Department of Aerospace Science and Technology, Politecnico di Milano, Via La Masa 34, Milano, Italy, luciaf.civati@polimi.it*
[f] *Department of Aerospace Science and Technology, Politecnico di Milano, Via La Masa 34, Milano, Italy, antonio.rizza@polimi.it*
[g] *Department of Aerospace Science and Technology, Politecnico di Milano, Via La Masa 34, Milano, Italy, carmine.giordano@polimi.it*
[h] *Department of Aerospace Science and Technology, Politecnico di Milano, Via La Masa 34, Milano, Italy, paolo.panicucci@polimi.it*
[i] *Department of Aerospace Science and Technology, Politecnico di Milano, Via La Masa 34, Milano, Italy, fabio1.ferrari@polimi.it*
[j] *Department of Aerospace Science and Technology, Politecnico di Milano, Via La Masa 34, Milano, Italy, francesco.topputo@polimi.it*
[*] *Corresponding author*

Abstract

The Hera mission will visit binary asteroid system Didymos to investigate the results of a kinetic impact with the smaller moonlet Dimorphos, successfully performed by the DART mission in 2022. On board Hera are two CubeSats, one being the Milani spacecraft. The use of CubeSats allows for more riskier operations, including closer flybys to the system. This results in high resolution imaging under different viewing geometries to be performed, which can complement the observations performed by Hera. The NavCam is the imager on board Milani, which is able to perform observation of the system using an RGB sensor in the visible wavelengths. Observations made by the NavCam will improve the estimate of the global properties of Didymos and Dimorphos, determine spectroscopic properties of the surface, and contribute to gravity field estimates with additional navigation observables and serendipitous particle tracking data. The observations made by the NavCam imager will aid the main objectives of the Hera mission, and additionally help inform both the scientific payload selection and navigation system design for future CubeSat missions to asteroids.

1. Introduction

The Asteroid Impact and Deflection Assessment (AIDA) collaboration, consisting of NASA's DART mission and ESA's Hera mission, aims to test the capability of a kinetic impactor to deflect an asteroid. At the end of September 2022, DART successfully impacted the secondary of the binary asteroid system Didymos, called Dimorphos [1] [2]. Hera will rendezvous with the binary system in late 2026, and plans to deploy two CubeSats in close-proximity of the asteroids [3]. Interplanetary CubeSats provide low-cost opportunities to extend the scientific and technological return of exploration missions. Hera's CubeSats, named Milani and Juventas, will be the first nanosatellites to orbit in the close proximity of a small celestial body performing scientific and technological operations around a binary asteroid [4].

Milani's main scientific objectives are: to characterize the surface and dynamical environment of both bodies, investigate the dust environment around the system, and provide measurements for determining the gravity field. Besides the scientific objectives, the Milani mission also aims to achieve several technological objectives related to testing environmental effects on key hardware and validating novel navigation algorithms. One of the payloads of Milani is the NavCam, an optical imager which nominally provides navigational information but will also be used to perform scientific investigations and perform experiments related to autonomous navigation around asteroids [27]. This imager contains an RGB filter that allows for spectrometric measurements, similar to the LUKE camera onboard the LICIACube spacecraft [5].

The DART mission has already provided a wealth of

information regarding the Didymos system and its physical properties [6–9]. Important characteristics like their shape, regolith properties, boulder properties, and bounds on the age of both bodies have been determined from these images. However, due to the limited viewing geometry, short observation period, and significant reshaping of Dimorphos after DART's impact [10], still multiple questions remain unanswered. As the Milani CubeSat will go closer to the system than the Hera spacecraft with a trajectory designed to specifically investigate the crater caused by DART [11], the observations from the NavCam will be essential to the general scientific goals of the mission.

This paper is structured as follows: first the Milani mission will be highlighted in section 2. Then, a more detailed description of the NavCam is given in section 3, followed by the main part of this paper in section 4, where the expected scientific investigations are discussed. Finally, concluding remarks are given in section 5.

2. Milani Mission

Milani is a 6U CubeSat that will be launched as a piggyback of the Hera spacecraft towards the Didymos binary system in 2024. After arriving at the system in 2027, Milani will be released from Hera and will focus on its scientific objectives, related to the characterization of Didymos' asteroids and their environment. The primary and secondary bodies of the system are called Didymos and Dimorphos (for simplicity, also referred to as D1 and D2). D1 is estimated to be an irregular-spherical-like body with a diameter of 780 m while D2 is modeled as a triaxial ellipsoid with a major axis of 170 m [12]. Milani's objectives are twofold: both scientific and technological. From a scientific point of view the main objectives are:

- **Study and characterize the Didymos binary system.** This includes support to Hera for the determination of the global properties of the system, characterization of the surface of both bodies, evaluation of space weathering phenomena, and characterization of surface properties near the crater.
- **Support the gravity field estimation.** This is achieved passively by the range and range-rate measurements exchanged between Milani and Hera via the ISL network during the entire mission. As will be discussed in section 4.3, the optical observables made by the NavCam will also aid in this investigation.
- **Characterization of the dust environment.** This includes the detection of inorganic materials, volatiles, and light organics within the asteroid environment and deep-space.

The scientific objectives are achieved by a global mapping of the two asteroids, high-resolution images of the crater on D2, surface micro-structure characterization of both bodies done with the NavCam payload and ASPECT payload [13], while radio-science and dust environment experiments are performed respectively with the ISL and the VISTA instrument [14]. From a technological point of view, Milani main objectives are:

- **Provide ISL communication with Hera.** This translates into the demonstration of the operability of an ISL network in deep-space.
- **Demonstrate the use of CubeSat technologies in deep-space.** This includes the capability to provide relative. positioning to Hera, to measure the effects of the asteroid environment on key hardware, and to validate autonomous navigation algorithms.

To accomplish both types of objectives, Milani is designed as a 6U CubeSat with orbital and attitude control capabilities. In addition to ASPECT, VISTA, and the ISL antennas, Milani will also host a lidar, sun-sensors a star-tracker, and an IMU. Milani's mission phases are schematized in Figure 1. The two main orbital phases of the mission are: the Far Range Phase (FRP) and Close Range Phase (CRP). The trajectory design process in the Didymos system is strongly influenced by the effect of gravitational and Solar radiation pressure perturbations and by the use of passive payloads (NavCam and ASPECT) [15, 16]. Because of this, Milani's proximity trajectories have been designed to fly above the Didymos system during FRP and CRP exploiting hyperbolic arcs, as illustrated in Figures 2a and 2b. The FRP and CRP last roughly 21 and 28 days respectively. As it is possible to see in Figure 2a, the FRP exhibits symmetrical arcs that develop within 8-14 km from D1 while the CRP, shown in Figure 2b exhibits asymmetrical arcs within 2-11 km. To conclude the mission after achievement of the main scientific objectives, the CRP will be followed by an Experimental Phase (EXP) shown in Figure 2c, which will climax in a landing attempt on eiher D1 or D2. In Figure 2d it is possible to see the values of the range to D1 and D2 during the COP, FRP, CRP, and EXP phases of the mission. The focus of this work is on the NavCam and the scientific observations it will perform. However, various works in the literature illustrate different aspects of the Milani missions. These are briefly listed here for the interested reader to provide context for what is presented in this work. The close-proximity trajectory design around a binary asteroid is discussed at length in [16] while the preliminary mission analysis and GNC design of Milani which constituted phase 0 of the mission is illustrated in [15, 27].

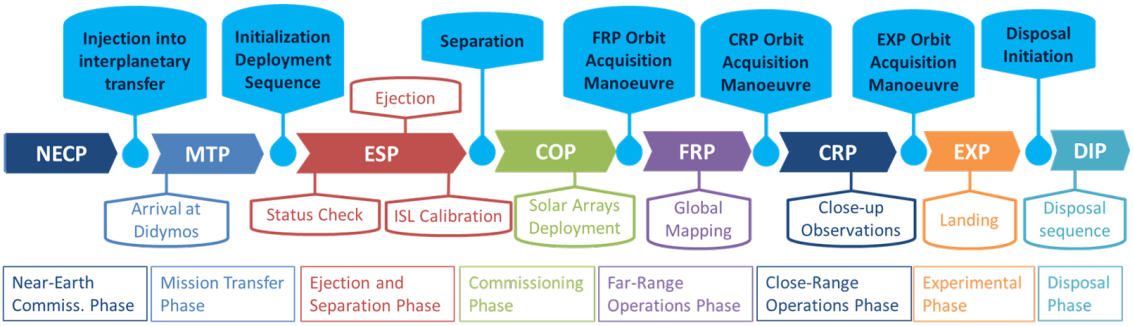

Fig. 1. The timeline of the Milani mission

In [11] the trajectory design and orbit determination processes are shown. The interested reader is directed to [13, 14] for details about VISTA and ASPECT, respectively.

The Milani consortium is composed by entities and institutions from Italy, Czech Republic and Finland. Consortium Prime is Tyvak International, responsible for the whole program management and platform design, development, integration, testing and final delivery to the customer. Politecnico di Torino is dealing with requirements definition, thermal analysis, radiation analysis and debris analysis. Politecnico di Milano is responsible for the NavCam payload, Mission Analysis, and GNC. Altec will support in the Ground Segment architecture and interfaces definition. Centro Italiano per la Ricerca Aerospaziale (CIRA) will be responsible for the execution of the vehicle environmental campaign. HULD will contribute in developing the mission-specific software. VTT is the main payload (ASPECT, spectral imager) provider, and is supported by the following entities dealing with ASPECT-related development: University of Helsinki (ASPECT calibration), Reaktor Space Lab (ASPECT Data Processing Unit development), Institute of Geology – the Czech Republic Academy of Science (ASPECT scientific algorithms requirements and testing), Brno University of Technology (ASPECT scientific algorithms development). INAF-IAPS is the secondary Payload (VISTA, dust detector) provider.

3. The NavCam Imager

The Navigation Camera is based on a Tyvak Star Tracker technology, customized for the Milani mission. Optical lenses were designed and coated specifically for Milani by Optec SpA. Tyvak ProxOps Vis Imgr WFOV Enhanced camera was selected as baseline for the mission, due to FOV constraints for the primary navigation camera, namely the requirement to keep the whole system in view at all mission ranges. A Jenoptik DLEM-30 LIDAR is also present on the satellite, and considering the relatively small range, it is complementary to the primary NavCam. In fact, it will mainly ease the relative navigation with respect to the target in the CRP and in the EXP, where the NavCam would be saturated by Didymos. Some of the most important properties of the NavCam are given in Table 1.

Table 1. Milani NavCam Properties.

Parameter	Value
Field of View [deg]	19.72 × 14.86
Field of View [m]	174 @500m distance 695 @2km distance 3476 @10km distance
Spectral range [nm]	400–700
Image size [pixels]	2048 x 1536
Pixel size [µm]	2.2 x 2.2
Focal length [mm]	12.96
Working distance [km]	30–0.2
Resolution [cm/px]	8.48 @ 500m distance 33.95 @ 2km distance 169.75 @ 10km distance

An important property of the NavCam is the fact that it has a Bayer filter RGB sensor (the Onsemi AR0331), which will provide color information in its images. The spectral response of the individual RGB channels is given in Figure 4. The NavCam largely overlaps with the wavelengths of the ASPECT imager, providing complementary measurements. However, there is also a region in the lower wavelengths (between 400 and 500 nm [13]) which ASPECT does not observe. Thus, the NavCam can pro-

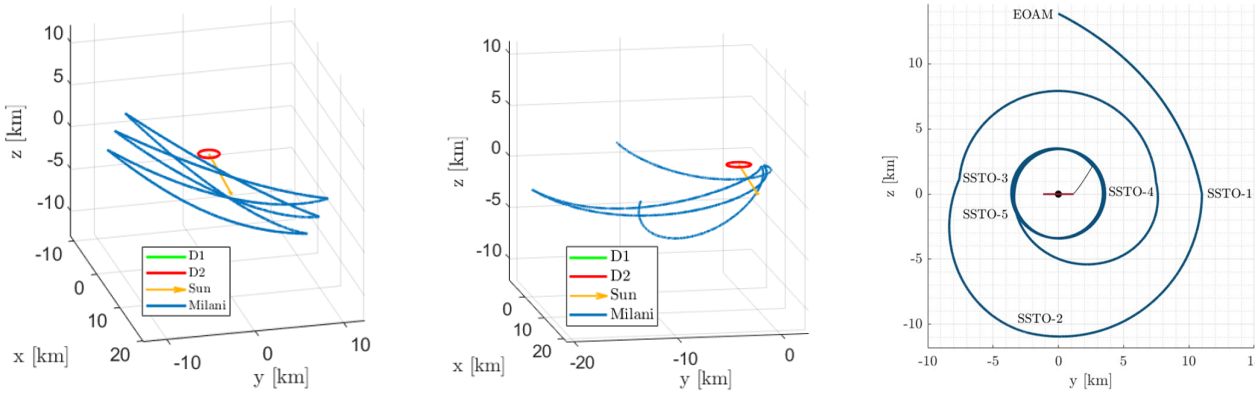

(a) FRP (b) CRP (c) EXP

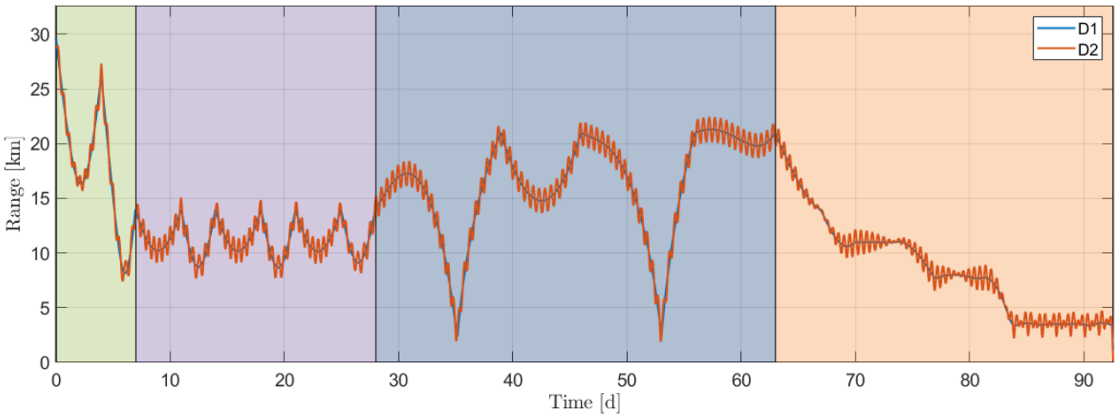

(d) The distance between Milani and D1 and D2 over time.

Fig. 2. The different mission phases of Milani.

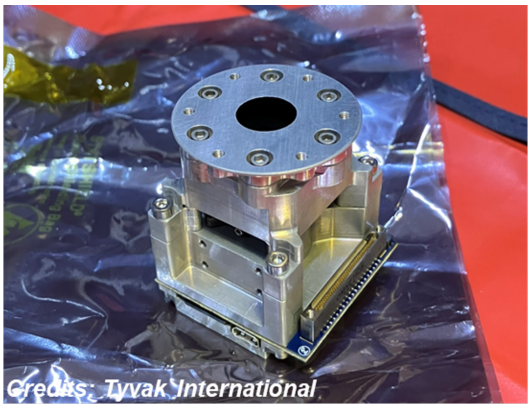

Fig. 3. The Milani NavCam imager with baffle.

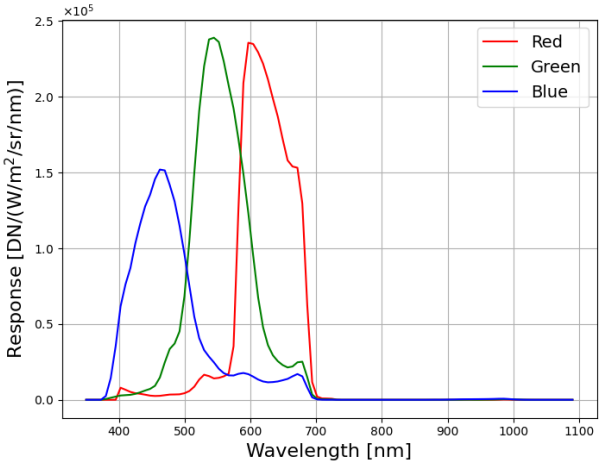

Fig. 4. The response curves of the different RGB channels of the NavCam. The QE represents the detector Quantum Efficiency, i.e. the amount of photons of a specific wavelength converted to measured electrons.

vide unique observation in terms of both wavelengths and geometry with respect to all other instruments on board Milani, Hera, and Juventas.

4. Expected Scientific Investigations

The NavCam will support the general scientific objectives of Milani as stated in section 2. Its close proximity and complimentary geometry with respect to Hera and Juventas will allow it to perform various scientific observations. The RGB sensor will also allow for several spectroscopic measurements to be performed. A general overview of the science traceability matrix (STM) associated with the NavCam is shown in Figure 5. The STM links the science objectives and goals set by the Milani mission in general, to the science and measurement requirements specific to the NavCam. In the next section these individual goals and objectves will be discussed in more detail.

4.1 Global Asteroid Properties

The global properties of Didymos and Dimorphos are macroscopic parameters like mass, shape, density, rotational state, and porosity, that physically define the system and its dynamical evolution. The shape of both Didymos and Dimorphos will allow for various scientific questions to be answered. Before the DART arrival, the shape of Didymos was thought to be very similar to asteroids Bennu and Ryugu, i.e. a top shaped asteroid. This raised the question of what processes guide the generation of these shapes, as their spectral types, and thus their composition, are different (B/C-type compared to S-type) [3]. The arrival of DART and the images taken by the DRACO camera revealed a shape that was significantly different than previously estimated [6], with a much more pronounced equatorial bulge and shorter length along the polar axis. The updated shape of Didymos can be seen in Figure 6a. The shape of Didymos, together with its measured rotation, has significant implications on the formation of binary asteroids as it can hint towards certain formation scenarios [17]. Obtaining high resolution maps of the full body (current shape model is biased in resolution towards the side that was observed by DRACO) will allow us to better infer how the shape of Didymos is linked to the formation of binary asteroids. Combining the shape with mass and interior measurements made by JuRa will also allow for density estimates of both Didymos and Dimorphos, better constraining their dynamical history and allows for estimating the similarities between the two bodies. A heterogeneous density distribution can also be measured by comparing the calculated gravity properties of a constant density model with the measured gravity field [18]. Another type of process that significantly impacts the evolution of (binary) asteroids is the (binary) Yarkovsky–O'Keefe–Radzievskii–Paddack ((B)YORP) effect [19], which alters the rotation and orbital state of the system over long periods of time due to thermal radiation. This effect is highly dependent on the shape of the asteroid, and thus a highly detailed shape model will improve our understanding of the precise influence of this effect on the evolution of this system. Finally, the shape of Dimorphos will likely be significantly altered due to the DART impact [10]. A detailed shape model of Dimorphos will allow for the determination of how effective the kinetic deflection exactly was, as it will reveal information on various properties of Dimorphos, e.g. internal strength, stiffness, internal structure, etc.

The NavCam will perform several different observa-

75th International Astronautical Congress (IAC), Milan, Italy, 14-18 October 2024.

Science Goal	Science Objective	Science Requirement	Measurement Requirement
The mission shall map the global composition of the Didymos asteroids.	To support the determination of the global properties of the Didymos asteroids.	The surface of the Didymos bodies shall be mapped to achieve at least a 90% global coverage, except areas which might be permanently shadowed during the mission.	The NavCam shall image Didymos with a spatial resolution better than 2m/pixel.
			The NavCam shall image Dimorphos with a spatial resolution better than 1m/pixel.
			The NavCam shall image the bodies at Sun phase angles between 5 and 25 deg.
		The shape of the Didymos asteroids shall be determined.	The NavCam images of the surface shall be taken at Sun incidence angles between 20 and 75 degrees, over a range of different azimuth angles.
			5 (TBC) overlapping images shall be taken with the NavCam for each maplet of the surface of the asteroids at a height where a GSD of at least 8 m/pixel is possible.
			For each maplet an albedo value shall be determined using a NavCam image at a Sun incidence angle < 7 degrees.
		The mission shall improve the rotational model of both asteroids.	See requirements for shape model determination.
			See requirements for gravity field determination.
The mission shall characterize the surface of the Didymos asteroids.	To characterize the spectral properties of the Didymos bodies surface.	The phase curves of selected areas of the surface shall be measured.	The NavCam shall image selected areas of the bodies with at least one observation at phase angles in the range of [0, 5] deg, at least one at phase angles in the range of [5, 10] deg, and at least three observations in the range of [10, 60] degrees.
		To compare mature and freshly exposed material at global scale.	The NavCam shall measure the surface in three different color bands (RGB) to determine the spectral properties of the fresh and mature materials.
The mission shall identify local shock effects on Dimorphos caused by DART.	To characterize the crater made by DART.	The diameter of the crater (if present) shall be measured.	The NavCam shall image the DART impact site with a resolution better than 0.5 m/pixel, with at least one observation at a phase angle in the range of [0, 10] deg and one observation at a phase angle of [30, 60] deg.
		The difference in shape, or any impact-produced surface feature, with respect to the pre-DART impact conditions shall be measured.	See requirements for the shape model.
The mission shall support Didymos gravity field determination	The mass measurement of both asteroids, and the accuracy of higher order gravity field parameters (J2 and higher) shall be improved.	The mission shall provide additional measurements to improve the gravity field determination of both bodies.	The NavCam shall track the centroid and surface feature to estimate the state of Milani with an accuracy of 1 m and 0.5 mm/s.
			The NavCam shall detect and track the motion of natural particles (if present) around the system.
			The NavCam shall image Juventas during its landing and on the surface of Dimorphos.

Fig. 5. The science traceability matrix of the NavCam scientific investigations.

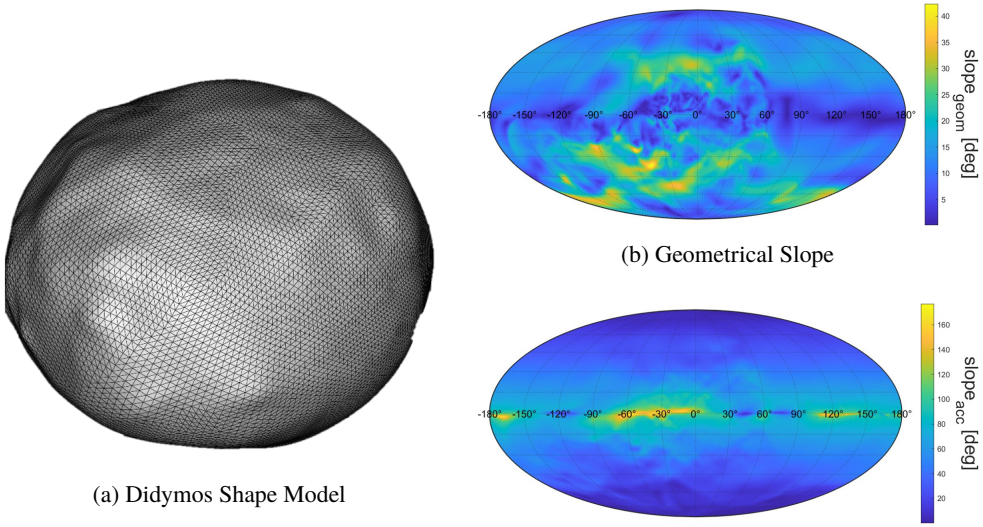

(a) Didymos Shape Model

(b) Geometrical Slope

(c) Geopotential Slope

Fig. 6. The shape and slopes of Didymos, taken from the latest shape model of Didymos from DART data [6].

tion that, together with the images from the other instruments, will lead to a detailed shape model. These models will be produced through a method called stereophotoclinometry (SPC) [20]. This technique combines observations made from the limb of the body when the body is not fully in the field of view of the camera, with images from individual maplets of the surface containing landmarks. These maplets, and their 3D position obtained through triangulation, are combined with the limb based data to generate a high resolution digital terrain model (DTM). A more in depth explanation of how this process precisely works is given in [21]. Using both the SPC method, and the tracked landmarks within the maplets, the rotational state of both bodies can also be estimated [22]. The different requirements on observation geometry for the NavCam are based on the optimal parameters for shape model generation through SPC.

4.2 Surface Characterization

The scientific observations of the surface will consist of two parts: its geomorphological properties and its spectral properties. Regarding the geomorphology, the first investigation that can be done is to look at the surface slopes of both bodies. A map of the surface slopes derived from the current shape model of Didymos can be found in Figure 6b. The slope map can be combined with the estimates of the rotational state and gravity field to obtain a geopotential slope map, which measures the angle between the (negative) surface normal and the local acceleration vector, see Figure 6c. By obtaining observations of regolith movement and slope destabilization, and correlating them with the slope maps, surface characteristics like: regolith properties, gravity anomalies, and density distribution discrepancies, can be estimated. For the spectral investigations, several different properties can be measured. First, lab tests have shown that shocking certain materials can have a large effect on their spectral properties, see Figure 7a. Obtaining information on the spatial distribution of shocked material will allow for a better understanding of what happened after the DART impact. Furthermore, shocked material can also indicate meteor impacts, providing information on the age of the system. Similar changes in spectra can be observed for weathered and unweathered material, see Figures 7b and 7c. Besides also helping in determining material that was recently exposed due to the DART impact it also allows for unprecedented investigations into the process of space weathering and how this affects the transport of different materials across the Solar-System [23]. Finally, measuring the compositional properties of the asteroid will allow for inferring a meteorite analogue of the system, which in turn will allow for better bulk density and porosity estimate.

The RGB sensor will allow for measuring the incoming light through three different filters, with their spectral response shown in Figure 4. To estimate how different RGB values relate to the composition of surface elements, the response first has to be simulated using lab data. For this, a database of spectra was used called RELAB [24]. This database contains a large amount of different minerals and meteorites, with also shock and space weathering experiment results present in the database. A set of these

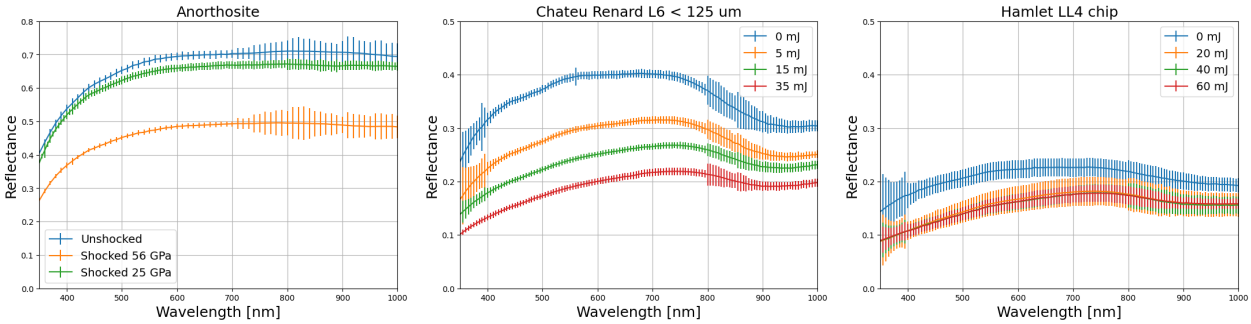

(a) Shocked Material Spectra (b) Weathered L6 Material Spectra (c) Weathered LL4 Material Spectra

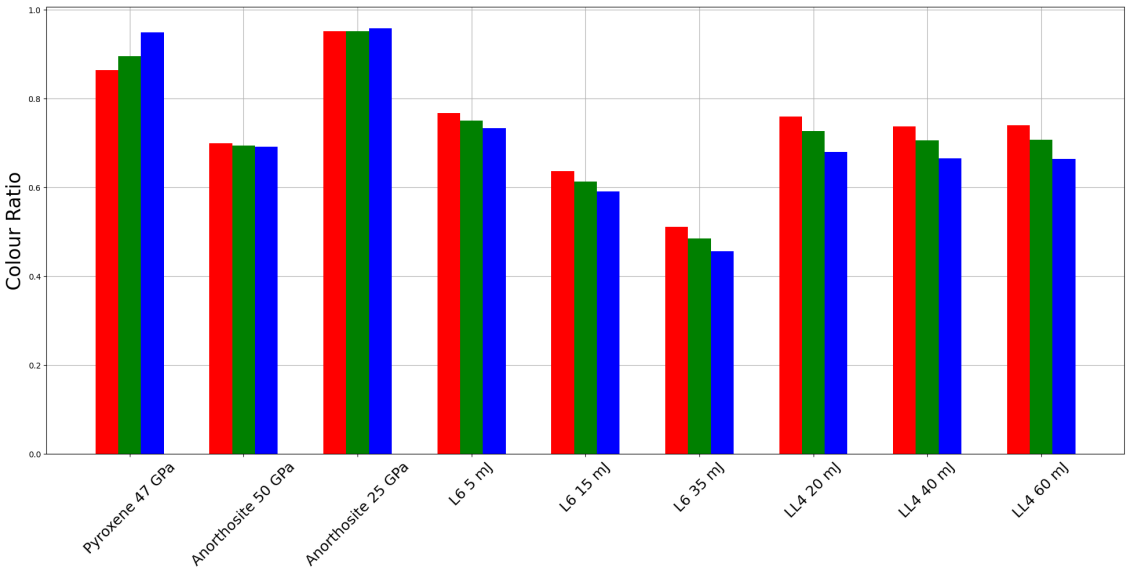

(d) RGB ratios.

Fig. 7. Different spectra for shocked Anorthosite and weathered L6 Chateau-Renard ordinary chondrite meteorite, and how the RGB values differ between unshocked/unweather and shocked/weathered material.

spectra with uncertainty bounds can be seen in Figures 7a - 7c. To simulate the RGB outputs from observing these materials, the spectra needs to be convoluted with the RGB sensor response curves as follows:

$$I_c = \int_{\lambda_{lb,c}}^{\lambda_{ub,c}} R_m(\lambda) R_c(\lambda) d\lambda, \qquad [1]$$

where I_c is the sensor reading for channel c, $\lambda_{lb,c}$ and $\lambda_{ub,c}$ are the channel's wavelength lower and upper bound, $R_m(\lambda)$ is the material spectrum, and $R_c(\lambda)$ is the channel's response function. An example of the shocked/unshocked and weathered/unweathered ratios for each of the RGB channels can be found for a set of different materials in Figure 7d. It can be seen that for all cases, the ratios are far from 1, meaning that with an RGB sensor these measurements can identify the differences between these materials. The measure of shock and weathering is in some cases also possible to infer, however this is not always the case as can be seen for the LL4 meteorite results.

Creating a database of materials and their respective RGB values will allow for the measurements of spatial distribution of these materials. A powerful statistical tool that has been used previously to investigate variations in surface composition across a body is called G-mode clustering [25]. It allows for the determination of homogeneous groups of objects within a larger population of objects described by a certain number of variables (e.g. here the objects are observations of certain locations on the surface and the descriptions are the RGB values). Thus, using this technique a set of regions on the body can be identified with similar spectral properties, for which the exact composition can be inferred from using the database of materials and their RGB values.

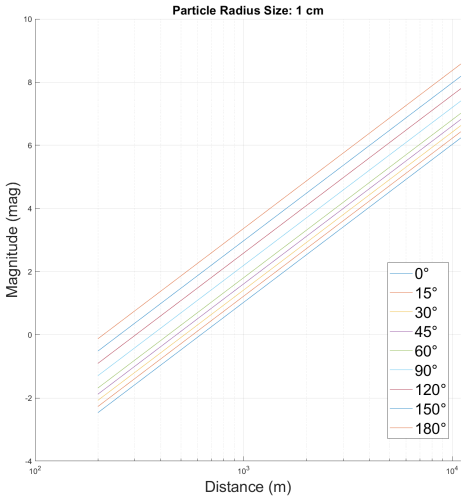

(a) 1 cm particles.

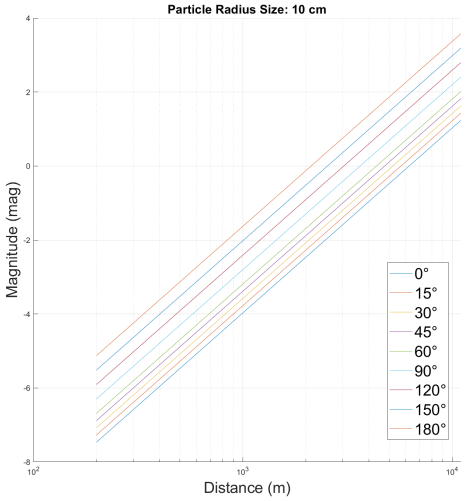

(b) 10 cm particles

Fig. 8. Apparent magnitude of different particle sizes.

4.3 Support Gravity Field Determination

As mentioned several times in sections 4.1 and 4.2, the gravity field generated by the asteroid is of great importance to various geophysical investigations of an asteroid. From it, information about the internal structure, surface morphology, and binary dynamics can be measured. The determination of the gravity field is of great importance to not only the scientific understanding of asteroids but also to the trajectory design of the spacecrafts.

The main gravity field determination will be performed by the radio science experiment (RSE), led by the University of Bologna [26]. This experiment will use radio tracking data from Earth, together with measurements from the inter-satellite link, to determine the position of Hera and the two CubeSats as they move around the system. Using orbit determination (OD) techniques this information can then be used to estimate the mass, rotational state, and higher order gravitational moments of both bodies. Reducing the uncertainty in the state estimates for the CubeSats will likely also improve the estimates in the gravity field of both bodies.

For the NavCam's role as navigational instrument, a set of image processing techniques have been developed to obtain observables from the images that can be used to track Milani's state over time [27]. These observables are mainly the centroid of the body, but other information sources like landmarks could also be retrieved during mission phases where Milani is close to the bodies.

The main limitation for the accuracy in the gravity field estimate is the amount of time the spacecraft spends close to the body where the influence of higher order harmon-

ics is more noticeable. During the OSIRIS-Rex mission, several natural particles were found around the asteroid [28]. These ejected particles could afterwards be tracked and together with the data from the state of the spacecraft, the gravity field of Bennu was improved from a 4th degree field to a 9th degree field. This significantly helped in the determination of the heterogeneous mass dsitribution inside Bennu [18, 29, 30]. The apparent magnitude of these particles for different phase angles and particle sizes can be seen in Figure 8, showing the feasibility of observing small ejecta using the Milani NavCam.

5. Conclusions

This work introduces the Milani mission and the NavCam imager, which will be used to perform scientific observations of the Didymos binary asteroid system. The alternate observation geometry with respect to Hera will allow for good synergy between the different spacecrafts, and improved accuracy in the measurements. Observations made by the NavCam will improve the estimate of the global properties of Didymos and Dimorphos, including shape, mass, and rotational state. It will also be able to determine spectroscopic properties of the surface, distinguishing between weathered and unweathered regions, and shocked and non-shocked regions. Finally, it will improve gravity field estimates by providing additional navigation observables and by looking for ejecta and tracking their trajectory as they move around the system.

These investigations will not only aid the investigation of the Didymos system during the Hera mission, but also show how CubeSat instruments can provide scientifically relevant information for asteroid missions in general.

Acknowledgements

The authors would like to acknowledge the full Milani team for their contribution to this paper.

References

[1] R. T. Daly *et al.*, "Successful kinetic impact into an asteroid for planetary defence," *Nature 2023 616:7957*, vol. 616, pp. 443–447, 7957 Mar. 2023, ISSN: 1476-4687. DOI: 10.1038/s41586-023-05810-5. [Online]. Available: https://www.nature.com/articles/s41586-023-05810-5.

[2] N. L. Chabot *et al.*, "Achievement of the planetary defense investigations of the double asteroid redirection test (dart) mission," *The Planetary Science Journal*, vol. 5, p. 49, 2 Feb. 2024, ISSN: 2632-3338. DOI: 10.3847/PSJ/AD16E6. [Online]. Available: https://iopscience.iop.org/article/10.3847/PSJ/ad16e6%20https://iopscience.iop.org/article/10.3847/PSJ/ad16e6/meta.

[3] P. Michel, M. Küppers, A. C. Bagatin, B. Carry, S. Charnoz, *et al.*, "The esa hera mission: Detailed characterization of the dart impact outcome and of the binary asteroid (65803) didymos," *The Planetary Science Journal*, vol. 3, p. 160, 7 Jul. 2022, ISSN: 2632-3338. DOI: 10.3847/PSJ/AC6F52. [Online]. Available: https://iopscience.iop.org/article/10.3847/PSJ/ac6f52%20https://iopscience.iop.org/article/10.3847/PSJ/ac6f52/meta.

[4] R. Walker *et al.*, "Deep-space CubeSats: thinking inside the box," *Astronomy and Geophysics*, vol. 59, no. 5, pp. 5.24–5.30, Oct. 2018. DOI: 10.1093/astrogeo/aty232.

[5] G. Poggiali *et al.*, "Expected investigation of the (65803) didymos–dimorphos system using the rgb spectrophotometry data set from the liciacube unit key explorer (luke) wide-angle camera," *The Planetary Science Journal*, vol. 3, p. 161, 7 Jul. 2022, ISSN: 2632-3338. DOI: 10.3847/PSJ/AC76C4. [Online]. Available: https://iopscience.iop.org/article/10.3847/PSJ/ac76c4%20https://iopscience.iop.org/article/10.3847/PSJ/ac76c4/meta.

[6] O. Barnouin *et al.*, "The geology and evolution of the near-earth binary asteroid system (65803) didymos," *Nature Communications 2024 15:1*, vol. 15, pp. 1–14, 1 Jul. 2024, ISSN: 2041-1723. DOI: 10.1038/s41467-024-50146-x. [Online]. Available: https://www.nature.com/articles/s41467-024-50146-x.

[7] J. Bigot *et al.*, "The bearing capacity of asteroid (65803) didymos estimated from boulder tracks," *Nature Communications 2024 15:1*, vol. 15, pp. 1–11, 1 Jul. 2024, ISSN: 2041-1723. DOI: 10.1038/s41467-024-50149-8. [Online]. Available: https://www.nature.com/articles/s41467-024-50149-8.

[8] M. Pajola *et al.*, "Evidence for multi-fragmentation and mass shedding of boulders on rubble-pile binary asteroid system (65803) didymos," *Nature Communications 2024 15:1*, vol. 15, pp. 1–13, 1 Jul. 2024, ISSN: 2041-1723. DOI: 10.1038/s41467-024-50148-9. [Online]. Available: https://www.nature.com/articles/s41467-024-50148-9.

[9] A. Lucchetti *et al.*, "Fast boulder fracturing by thermal fatigue detected on stony asteroids," *Nature Communications 2024 15:1*, vol. 15, pp. 1–11, 1 Jul. 2024, ISSN: 2041-1723. DOI: 10.1038/s41467-024-50145-y. [Online]. Available: https://www.nature.com/articles/s41467-024-50145-y.

[10] S. D. Raducan *et al.*, "Physical properties of asteroid dimorphos as derived from the dart impact," *Nature Astronomy 2024 8:4*, vol. 8, pp. 445–455, 4 Feb. 2024, ISSN: 2397-3366. DOI: 10.1038/s41550-024-02200-3. [Online]. Available: https://www.nature.com/articles/s41550-024-02200-3.

[11] C. Bottiglieri, F. Piccolo, C. Giordano, F. Ferrari, and F. Topputo, "Applied trajectory design for cubesat close-proximity operations around asteroids: The milani case," *Aerospace 2023, Vol. 10, Page 464*, vol. 10, p. 464, 5 May 2023, ISSN: 2226-4310. DOI: 10.3390/AEROSPACE10050464. [Online]. Available: https://www.mdpi.com/2226-4310/10/5/464/htm%20https://www.mdpi.com/2226-4310/10/5/464.

[12] R. T. Daly *et al.*, "An updated shape model of dimorphos from dart data," *The Planetary Science Journal*, vol. 5, p. 24, 1 Jan. 2024, ISSN: 2632-3338. DOI: 10.3847/PSJ/AD0B07. [Online]. Available: https://iopscience.iop.org/article/10.3847/PSJ/ad0b07%20https://iopscience.iop.org/article/10.3847/PSJ/ad0b07/meta.

[13] T. Kohout, M. Cardi, A. Näsilä, E. Palomba, and F. Topputo, "Milani cubesat for esa hera mission," in *Europlanet Science Congress*, Copernicus Meetings, Jun. 2021. DOI: 10.5194/EPSC2021-732. [Online]. Available: https://meetingorganizer.copernicus.org/EPSC2021/EPSC2021-732.html.

[14] F. Dirri *et al.*, "Vista instrument: A pcm-based sensor for organics and volatiles characterization by using thermogravimetric technique," *5th IEEE International Workshop on Metrology for AeroSpace, MetroAeroSpace 2018 - Proceedings*, pp. 150–154, Aug. 2018. DOI: 10.1109/METROAEROSPACE.2018.8453532.

[15] F. Ferrari, V. Franzese, M. Pugliatti, C. Giordano, and F. Topputo, "Preliminary mission profile of hera's milani cubesat," *Advances in Space Research*, vol. 67, pp. 2010–2029, 6 Mar. 2021, ISSN: 0273-1177. DOI: 10.1016/J.ASR.2020.12.034.

[16] F. Ferrari, V. Franzese, M. Pugliatti, C. Giordano, and F. Topputo, "Trajectory options for hera's milani cubesat around (65803) didymos," *Journal of the Astronautical Sciences*, vol. 68, pp. 973–994, 4 Dec. 2021, ISSN: 21950571. DOI: 10.1007/S40295-021-00282-Z/FIGURES/11. [Online]. Available: https://link.springer.com/article/10.1007/s40295-021-00282-z.

[17] J. Wimarsson *et al.*, "Rapid formation of binary asteroid systems post rotational failure: A recipe for making atypically shaped satellites," *Icarus*, vol. 421, p. 116 223, Oct. 2024, ISSN: 0019-1035. DOI: 10.1016/J.ICARUS.2024.116223.

[18] D. J. Scheeres *et al.*, "Heterogeneous mass distribution of the rubble-pile asteroid (101955) bennu," *Science Advances*, vol. 6, 41 Oct. 2020, ISSN: 23752548. DOI: 10.1126/SCIADV.ABC3350/SUPPL_FILE/ABC3350_SM.PDF. [Online]. Available: https://www.science.org/doi/10.1126/sciadv.abc3350.

[19] M. Ćuk *et al.*, "Byorp and dissipation in binary asteroids: Lessons from dart," *The Planetary Science Journal*, vol. 5, p. 166, 7 Jul. 2024, ISSN: 2632-3338. DOI: 10.3847/PSJ/AD5D5E. [Online]. Available: https://iopscience.iop.org/article/10.3847/PSJ/ad5d5e%20https://iopscience.iop.org/article/10.3847/PSJ/ad5d5e/meta.

[20] C. D. Adam *et al.*, "Stereophotoclinometry for osiris-rex spacecraft navigation," *The Planetary Science Journal*, vol. 4, p. 167, 9 Sep. 2023, ISSN: 2632-3338. DOI: 10.3847/PSJ/ACE31D. [Online]. Available: https://iopscience.iop.org/article/10.3847/PSJ/ace31d%20https://iopscience.iop.org/article/10.3847/PSJ/ace31d/meta.

[21] E. E. Palmer, R. Gaskell, M. G. Daly, O. S. Barnouin, C. D. Adam, and D. S. Lauretta, "Practical stereophotoclinometry for modeling shape and topography on planetary missions," *The Planetary Science Journal*, vol. 3, p. 102, 5 May 2022, ISSN: 2632-3338. DOI: 10.3847/PSJ/AC460F. [Online]. Available: https://iopscience.iop.org/article/10.3847/PSJ/ac460f%20https://iopscience.iop.org/article/10.3847/PSJ/ac460f/meta.

[22] P. Panicucci, J. Lebreton, R. Brochard, E. Zenou, and M. Delpech, "Vision-based estimation of small body rotational state," *Acta Astronautica*, vol. 213,

pp. 177–196, Dec. 2023, ISSN: 0094-5765. DOI: 10.1016/J.ACTAASTRO.2023.08.046.

[23] B. E. Clark *et al.*, "Overview of the search for signs of space weathering on the low-albedo asteroid (101955) bennu," *Icarus*, vol. 400, p. 115 563, Aug. 2023, ISSN: 0019-1035. DOI: 10.1016/J.ICARUS.2023.115563.

[24] C. M. Pieters and T. Hiroi, "RELAB (Reflectance Experiment Laboratory): A NASA Multiuser Spectroscopy Facility," in *Lunar and Planetary Science Conference*, S. Mackwell and E. Stansbery, Eds., ser. Lunar and Planetary Science Conference, Mar. 2004, p. 1720.

[25] D. Perna *et al.*, "Multivariate statistical analysis of osiris/rosetta spectrophotometric data of comet 67p/churyumov-gerasimenko," *Astronomy & Astrophysics*, vol. 600, A115, Apr. 2017, ISSN: 0004-6361. DOI: 10.1051/0004-6361/201630015. [Online]. Available: https://www.aanda.org/articles/aa/full_html/2017/04/aa30015-16/aa30015-16.html%20https://www.aanda.org/articles/aa/abs/2017/04/aa30015-16/aa30015-16.html.

[26] E. Gramigna *et al.*, "The hera radio science experiment at didymos," *Planetary and Space Science*, vol. 246, p. 105 906, Jul. 2024, ISSN: 0032-0633. DOI: 10.1016/J.PSS.2024.105906.

[27] M. Pugliatti, F. Piccolo, A. Rizza, V. Franzese, and F. Topputo, "The vision-based guidance, navigation, and control system of hera's milani cubesat," *Acta Astronautica*, vol. 210, pp. 14–28, Sep. 2023, ISSN: 0094-5765. DOI: 10.1016/J.ACTAASTRO.2023.04.047.

[28] S. R. Chesley *et al.*, "Trajectory estimation for particles observed in the vicinity of (101955) bennu," *Journal of Geophysical Research: Planets*, vol. 125, e2019JE006363, 9 Sep. 2020, ISSN: 2169-9100. DOI: 10.1029/2019JE006363. [Online]. Available: https://onlinelibrary.wiley.com/doi/full/10.1029/2019JE006363%20https://onlinelibrary.wiley.com/doi/abs/10.1029/2019JE006363%20https://agupubs.onlinelibrary.wiley.com/doi/10.1029/2019JE006363.

[29] R. A. Werner, "The gravitational potential of a homogeneous polyhedron or don't cut corners," *Celestial Mechanics & Dynamical Astronomy*, vol. 59, pp. 253–278, 3 Jul. 1994, ISSN: 09232958. DOI: 10.1007/BF00692875. [Online]. Available: https://link.springer.com/article/10.1007/BF00692875.

[30] P. Panicucci *et al.*, "Uncertainties in the gravity spherical harmonics coefficients arising from a stochastic polyhedral shape," *Celestial Mechanics and Dynamical Astronomy*, vol. 132, p. 23, 4 Apr. 2020, ISSN: 15729478. DOI: 10.1007/s10569-020-09962-8. [Online]. Available: https://doi.org/10.1007/s10569-020-09962-8.